Journal of Hazardous Materials 167 (2009) 835–845

Contents lists available at ScienceDirect

Journal of Hazardous Materials

journal homepage: www.elsevier.com/locate/jhazmat

Trace element transformations and partitioning during the roasting of pyrite ores in the sulfuric acid industry

Chunxia Yang[a,b], Yongheng Chen[a,*], Ping'an Peng[b], Chao Li[b,1], Xiangyang Chang[a], Yingjuan Wu[a]

[a] School of Environmental Science and Engineering, Guangzhou University, Guangzhou 510405, PR China
[b] State Key Laboratory of Organic Geochemistry, Guangzhou Institute of Geochemistry, Chinese Academy of Sciences, Guangzhou 510640, PR China

ARTICLE INFO

Article history:
Received 24 April 2008
Received in revised form
20 November 2008
Accepted 15 January 2009
Available online 3 March 2009

Keywords:
Trace elements
Pyrite roasting wastes
Flue gas
Fluidized-bed furnace

ABSTRACT

Total concentrations combined with chemical partitioning of trace elements (Cd, Co, Cr, Mn, Ni, Pb, Tl, and Zn) in raw pyrite ore and solid roasting wastes were investigated in order to elucidate their transformations and partitioning during the roasting of raw pyrite ores in sulfuric acid production. In order to better understand the behavior of these elements during roasting, mineral transformations accompanying roasting were also investigated by using microscopy. Results indicated that the mode of occurrence of trace elements in raw pyrite ore and the thermostability of trace element-bearing species formed during roasting played major roles in the transformations of the selected trace elements. Silicate- and amorphous iron (hydr)oxide-bound elements (Cr and Pb) were stable and mainly retained in their original phases. However, acid-exchangeable and sulfide-bound elements tended to transform into other forms via different pathways: elements that tend to form low thermostable species (Cd, Pb and Tl) were significantly vaporized, whereas elements that tend to form high thermostable species (Co, Mn and Ni) mainly reacted with iron oxides or silicates, which then remained in the solid residues. The volatility of trace elements during the roasting has a significant effect on their subsequent partitioning in roasting wastes. Nonvolatile element (Co, Cr, Mn, and Ni) partitioning was determined by settling of the particulate in which they are bound, whereas the partitioning of (semi)volatile elements (Cd, Pb, Tl, and Zn) was controlled by the adsorption of their gaseous species on the particulate.

1. Introduction

Pyrite ore (FeS_2) has been widely used in modern industry for the production of sulfuric acid. Pyrite ore usually contains a wide range of trace elements, such as Cd, Co, Cr, Mn, Ni, Pb, Tl, and Zn [1]—some of which are highly toxic (e.g., Cd, Pb, Tl). During pyrite ore roasting, a series of physicochemical transformations occurs [2,3], resulting in potential dispersion of these trace elements from roasting wastes into the environment [4]. Several studies have shown that trace elements can be readily released into surrounding soil, water and sediment from the pyrite ore roasting wastes, posing potential threats to the environment [5–9]. It is essential to understand the transformations and partitioning of these trace elements during pyrite ore roasting, particularly in industrial settings, in order to control the potential pollution from the headstream. Unfortunately, a void in the literature exists regarding trace element behavior during pyrite ore roasting although the process of pyrite oxidation has been well studied (e.g., [2,3]).

The behaviors of trace elements during other thermal treatments (e.g., coal combustion, sewage sludge combustion) have been investigated by many studies [10–13]. Trace elements may be distributed to several output streams during thermal treatments, including solid residues and flue gas which enters a downstream pollution control device; elements in the flue gases may be present in the vapor phase or bound on fine particles [14]. Trace elements have been classified into three broad groups according to their partitioning behavior during combustion [14–16]. Group-I elements (nonvolatile elements) are concentrated in coarse residues or equally partitioned between coarse residues and fine particles. Group-II elements (semivolatile elements) are vaporized in the combustor but condense downstream and generally show enrichment with decreasing fly ash particle size due to elemental vaporization-ash surface deposition processes. Group-III elements (volatile elements) are the most volatile elements and are depleted in all solid phases. The extent of vaporization and subsequent deposition of these trace elements during the thermal treatments were believed to depend on the thermal treatment conditions (e.g., temperature, atmosphere condition, etc.), on the mode of occurrence

* Corresponding author. Tel.: +86 20 39366013; fax: +86 20 39366168.
E-mail address: chenyheng@eyou.com (Y. Chen).
[1] Present address: Department of Earth Sciences, University of California-Riverside, CA 92521, USA.

0304-3894/$ – see front matter © 2009 Elsevier B.V. All rights reserved.
doi:10.1016/j.jhazmat.2009.01.067

of the trace elements in raw materials, and on the physical changes and chemical reactions of these elements with sulfur and other compounds during combustion [17–20].

Due to high concentrations of pyrite as well as gangue minerals in raw materials, pyrite ore roasting during sulfuric acid production in an atmospheric fluidized-bed combustion system is characterized by the production of a large quantity of roasting wastes enriched with iron oxides and silicates, and a high concentration of sulfur compounds in flue gas; none of which is present in other thermal treatments, such as coal, wood bark or other combustions [17–20]. In order to determine whether there any differences between trace element behavior during pyrite ore roasting and other thermal treatments, and to provide essential knowledge regarding headstream control of related industrial pollution, we conducted an extensive survey of the concentrations and the mode of occurrence of trace elements (Cd, Co, Cr, Mn, Ni, Pb, Tl and Zn) in raw pyrite ores, bottom slag and fly ashes from a real sulfuric acid plant.

2. Experimental

2.1. Sampling

Sampling was carried out in a typical sulfuric acid plant in China—the Yunfu Sulfuric Acid Plant. Acid Plant located in Guangdong province which produces sulfuric acid from pyrite ore since 1985. We chose Yunfu sulfuric acid plant for sampling because unlike other sulfuric acid plants in China, this plant uses only ores from Yunfu pyrite mine. Thus, we avoid the possibility that the pyrite ore samples we collected might not represent the raw materials, which produced the observed partitioning in the downstream zone. In the Yunfu plant, raw materials are crushed (grain size <3–4 mm) before roasting in the fluidized-bed furnace (850 °C) for generating SO_2 (Fig. 1). The produced SO_2 is then purified through three-step precipitations in a boiler, a cyclone scrubber and a tower washer at 450, 300 and <60 °C, respectively, before being oxidized to SO_3, which is finally used for producing sulfuric acid (Fig. 1).

Samples of roasting waste were collected from fluidized-bed furnace bottom slag (FS), boiler fly ash (BA), cyclone scrubber fly ash (CA) and tower washer fly ash (WA). WA was obtained by removing the wastewater by centrifuging at 2000 rpm for 15 min. Pyrite ores were collected and analyzed for comparison. All of the samples were collected using a stainless steel shovel (except WA) and kept in polyethylene containers until analyses. Notably, we continuously collected the slag and fly ash samples from running devices in about an hour. Therefore, our slag and fly ash samples should come from the same raw materials, and are valid for the study of trace element transformation and migration in industrial production of sulfuric acid. Moreover, large-size slag grains in the FS, which were formed from the melting of the slag, were not collected in order to avoid heterogeneity in the samples. In the Yunfu Plant, the inner walls of the furnace and combustion chambers are lined with aluminosilicate firebrick. No contamination from, or catalytic reactions associated with, the aluminosilicate firebrick were observed to significantly affect the partitioning of trace elements in collected samples (see details in Section 3) and related literature. In addition, the plant annually generates about 40,000–75,000 tons of roasting wastes. Therefore, if there is any pre-existing contamination derived from the reactor parts it must have been much diluted.

The pyrite ore and FS samples were milled and ground to <250 μm prior to chemical analyses. The fly ash samples (BA, CA and WA) were analyzed without prior grinding.

2.2. Characteristics analysis

The mineralogy of pyrite ores and roasting wastes was investigated by MPV3 microscope. Grain size distribution of roasting wastes was measured by using combined sieve (>0.1 mm) and microscopic observation (<0.1 mm). Sulfur concentrations in pyrite ore and waste samples were measured by using weight method. Details for these methods can be found in Yang et al. [8].

2.3. Reagent

Double-deionized water (Milli-Q Millipore 18.3 MΩ/cm resistivity) was used for all experiments. All glassware used for the experiments were soaked in 14% HNO_3 (v/v) and rinsed with deionized water prior to use. Superpure nitric acid, hydrofluoric acid, perchloride acid, hydrogen peroxide, and analytical grade acetic acid (CH_3COOH), hydroxylammonium chloride ($NH_2OH{\cdot}HCl$) and ammonium acetate (CH_3COONH_4) were used for sequential extractions and total digestion as described below.

2.4. Total digestion

Total digestions of pyrite ore and roasting wastes were conducted according to the following procedures for determining the total concentrations of studied trace elements. About 30 mg of sample was placed in a platinum crucible and moistened with a few drops of water. Three ml concentrated HNO_3 and 15 mL HF were added to the crucible and the sample was swirled until completely wetted. The samples were then digested on a hot plate at 120 °C

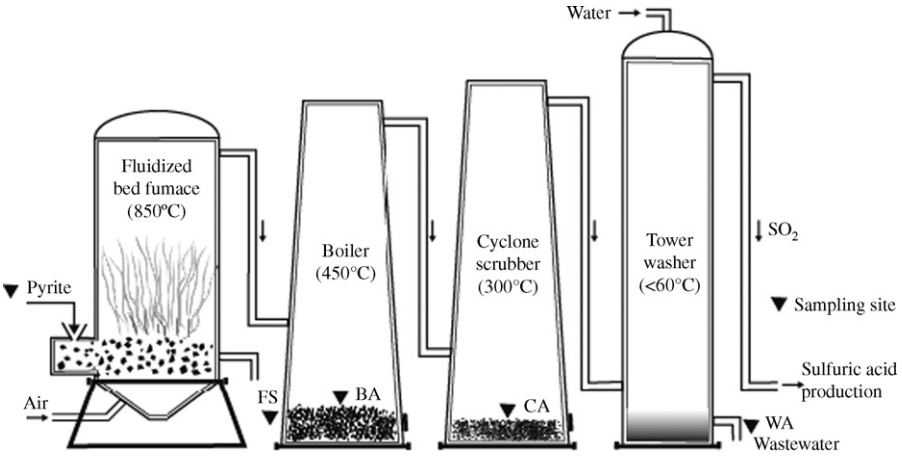

Fig. 1. Conceptual diagram of SO_2 production and purification in the Yunfu sulfuric acid plant. Sampling locations are denoted by filled triangles. FS: fluidized-bed furnace bottom slag; BA: boiler fly ash; CA: cyclone scrubber fly ash; WA: tower washer fly ash.

in open air until near dryness; a second addition of HF (15 mL) was made and the mixture was evaporated to near dryness again. Finally, concentrated $HClO_4$ (3 mL) was added and the sample was evaporated on the hot plate at 200 °C until near dryness. This step was repeated. The residues from the $HClO_4$ digestion were dissolved by using 2 mL 8 mol/L HNO_3 at low temperature and the sample was brought to a final volume of 100 mL with water. Each sample was stored in a capped polyethylene bottle at 4 °C for subsequent instrumental determination. Clear solutions were obtained for all samples. Blanks were carried out through the same procedures as the samples.

Limit of detection (LOD) for the total digestion analyses was calculated based on 10 repeated analyses of procedural blank and the result was normalized to the sample mass of 30 mg. The average LODs (3 s) for the total digestion analyses in this study are 1.0–16 ng/g for Cd, Co, Mn, Tl and 71–136 ng/g for Cr, Ni, Pb, Zn. A natural standard reference soil (GBW07406) from the National Research Center of China for Certified Reference Materials (NRCC-CRM) was prepared for trace element quantification in the same manner as the samples. The accuracy and the repeatability of the total digestion analyses were evaluated by triplicate analyses of four certified reference soils (NRCC-CRM GBW07401, 02, 03, and 05). The coefficients of variation (CVs) of the trace element analyses were less than 10% for the four reference soils. The accuracy obtained for the reference materials are within ±15% which is well within the accepted range of trace elements analyses using inductively coupled plasma mass spectrometry (ICP-MS) [21,22].

2.5. Sequential extraction

The sequential extraction procedure used in this study for determining the partitioning of studied trace elements in raw pyrite ores and roasting wastes was based on the standard method proposed by the Community Bureau of Reference (BCR) [23] but modified to be suitable for pyrite ore, slag and fly ash [8,24]. The extraction steps and conditions are summarized in Table 1. For a brief explanation of the mode of occurrence of trace elements extracted in each step:

Step 1: Acid-exchangeable (Exc). Trace elements extracted in this step include trace elements adsorbed on the raw pyrite ore or roasting waste surfaces via relatively weak electrostatic interaction, trace elements that can be released by ion-exchange processes, and acid-soluble trace element salts such as carbonates and sulfates.

Table 1
Modified BCR sequential extraction procedure used in this study (for 0.3 g sample).

Step	Extraction conditions	Nominal target phase (s)
1	20 mL CH_3COOH (0.11 mol/L, pH 2.8), 25 °C, 16 h, continual agitation	Exchangeable, water and acid soluble species
2	20 mL $NH_2OH{\cdot}HCl$ (0.5 mol/L, acidified to pH 1.5 with nitric acid), 25 °C, 16 h, continual agitation	Reducible species, e.g., bound to iron/manganese (hydr)oxides
3	5 mL H_2O_2 (8.8 mol/L), covered, 25 °C, 1 h; 85 °C in a water bath, 1 h; uncovered and evaporated to a small volume; repeated with a second volume of H_2O_2; 25 mL CH_3COONH_4 (1.0 mol/L, adjusted to pH 2.0 with nitric acid), 25 °C, 16 h, continual agitation	Oxidisable species, e.g., bound to sulfides
4	HNO_3-HF-$HClO_4$, same as the total digestion (see Section 2.4)	Residual species, e.g., bound to silicates or crystalline iron oxides

Step 2: Easily reducible (Red). Trace elements extracted in this step include trace elements bound to amorphous or poorly crystalline iron/manganese (hydr)oxides which are unstable under reducing conditions. Changing the redox potential (Eh) can induce the dissolution of these (hydr)oxides (e.g., limonite) and release their bound trace elements.

Step 3: Oxdizable (Oxi). Trace elements extracted in this step include trace elements bound to sulfides and organic matter. In this study, trace elements released in this step are mainly derived from the sulfide-associated fraction because of the extremely high pyrite concentration in the raw ore and significant residual sulfides in the roasting wastes.

Step 4: Residual (Res). Trace elements extracted in this step include those trace elements held within mineral crystalline matrix, which are not likely to be released under normal environmental conditions. The minerals mainly include naturally occurring silicates/crystalline minerals in the pyrite ore or roasting wastes, or newly formed crystalline minerals, such as iron oxides (e.g., hematite, magnetite) in the roasting wastes.

After each extraction step, the acquired suspension was centrifuged at 5000 r/min for 15 min and the supernatant was collected with a pipette. The residue was washed with 10 ml of water and centrifuged for 15 min, and then this second supernatant was collected and combined with the first supernatant. One ml of 16 mol/L HNO_3 was added into the combined supernatant, which was then evaporated close to dryness. One-fifth ml 8 mol/L HNO_3 was added and the volume was subsequently diluted to 10 mL with water. Blanks were prepared by the same procedure as the actual samples. All extracts obtained were stored in capped polyethylene bottles at 4 °C until being analyzed by ICP-MS.

Limit of detection (LOD) of the sequential extraction was calculated based on 10 repeated analyses of procedural blank and the result was normalized to the sample mass of 0.3 g. The LODs (3 s) of four sequential extraction steps are 0.57–14.9 ng/g for Cd, Co and Tl, 10.6–34.5 for Ni, and 6–250 ng/g for Cr, Mn, Zn and Pb. In order to evaluate the uncertainties of the sequential extraction procedure used for the selected trace elements, four replicate sets of two test samples were taken through the extraction procedure and analyzed. One of the test samples is a sample of soil contaminated by the sulfuric acid plant, while the other is a mixture of slag and fly ash waste also collected from the sulfuric acid plant; both of them have a similar range of trace element contents to our studied samples. The results show that the CVs of selected trace elements for step 1–4 are mostly less than 15%; higher CVs (20–40%) were only found in step 4.

The recovery of an element can be determined by comparing the sum of the element extracted by all extraction steps with its total digestion concentration: (sum/total) × 100. The mean recovery for single trace element in actual samples was between 90% and 117% except for Cr which has a mean recovery of 79%. The mean and median recoveries for all studied trace elements in actual samples were 97% and 96%, respectively. Compared to roasting wastes, pyrite ore samples have a relatively wide range of recoveries of selected trace elements probably due to the heterogeneity of the pyrite ore samples. Our recoveries of sequential extraction in the present work are similar to or better than those reported in available literature [25–29] where BCR sequential extraction of trace elements was also used.

2.6. Instrumental analyses

The analyses of trace elements from the total digestion and the sequential extraction were performed on an Elan 6000 ICP-MS (PerkinElmer, USA) [8]. Rhodium was used as the internal standard to eliminate short time variability and matrix effects during

Table 2
Mineralogy and grain size of pyrite ores, wall rocks and roasting wastes.

	Mineralogy[a]						Grain size (%)				
	Wall rocks	Pyrite ores	FS	BA	CA	WA		FS	BA	CA	WA
Pyrite	+	++++					>2 mm	30	0	0	0
Pyrrhotite			+	+	+		2–1 mm	22	0	0	0
Hematite			+++	+++	+++	+++	1–0.5 mm	17	0	0	0
Magnetite			+++	+++	+++	+++	0.5–0.3 mm	6	0	0	0
Limonite		+	+	+	+		0.3–0.1 mm	17	10	0	0
Quartz	++++	+	+++	++	++	++	0.1 mm–50 μm	8	55	20	5
Carbonate	+	+					50–10 μm	0	25	65	20
Clay	++	+	+++	++	++	++	<10 μm	0	10	15	75
Gypsum			+	+							

[a] Relative abundance: ++++, very abundant; +++, abundant; ++, minor; +, trace.

measurement [30]. The detailed analytical conditions can be found in references [8] and [24]. The concentrations of major elements were determined by using a PerkinElmer PE 3100 atomic absorption spectrometer for Na, Mg, K, Ca and Fe, and by using spectrophotometry for Al and Si.

3. Results and discussion

3.1. Mineral transformations during the roasting of pyrite ores

In order to better understand the behavior of trace elements during the roasting of pyrite ores, the mineral transformations that accompany pyrite roasting were mainly investigated by using microscopic observations and major element analyses. The mineral compositions and grain size distribution (for roasting wastes), and major element contents of raw pyrite ores, wall rocks and roasting wastes are summarized in Tables 2 and 3, respectively.

Raw materials used in Yunfu sulfuric acid plant were mainly composed of pyrite-rich ore (15–42% pyrite; 8–22% sulfur) and pyrite concentrate (88–99% pyrite; >51% sulfur) with minor wall rock contributions. Pyrite was the main mineral in the raw materials. Other minerals, such as quartz, clay, carbonate and limonite, only accounted for minor amounts in the pyrite concentrate, but were abundant in the pyrite-rich ore, wall rocks and gangues [31]. Accordingly, the relative abundances of gangue minerals in the raw materials could have been significantly elevated when more pyrite-rich ores than pyrite concentrates were used in the sulfuric acid production [31,32]. Under microscope, FS and fly ashes demonstrated roughly similar mineral compositions: ~50–70% of iron oxides (magnetite, hematite and limonite), ~20–40% of silicates (quartz, clays or aluminosilicates), <5% of residual sulfides (pyrrhotite) and trace amounts of gypsum. The presence of residual sulfides in the waste products analyzed by this study suggests that pyrite in the raw materials was not completely oxidized in the fluidized-bed furnace. As proposed by Srinivasachar et al. [2] and Hu et al. [3], in the case of incomplete combustion, pyrite will initially decompose to form pyrrhotite (FeS_x), which subsequently melts to form iron oxysulfide droplets, from which magnetite (Fe_3O_4) crystallizes out to finally form hematite (Fe_2O_3). As shown below, the specific structure and morphology of the iron oxide particles examined in this study support this proposition.

Although microscopic observations suggested that iron oxides had similar abundances in both FS and fly ashes, quantitative analyses of Fe concentrations indicated that iron oxides were more abundant in the fly ashes than in the FS (Table 3). Grain size analyses showed that grain size decreases from FS to WA (Table 2), suggesting that the iron oxides formed fine particles during roasting and were migrated with the flue gas. Detailed microscopic examination indicated that three main types of iron oxide particle remained in the wastes: A-type—partially oxidized pyrite particles surrounded by a porous pyrrhotite (FeS_x) and magnetite (Fe_3O_4) mixture layer and a hematite (Fe_2O_3) rim; B-type—completely decomposed pyrite particles with massive fissures; and C-type—angular, fine iron oxide particles. Mineral compositions of B- and C-type particles are mainly magnetite and hematite. Particle size analysis demonstrated that the A-, B- and C-types of iron oxide particles are generally in the sizes of >150, 50–150 and <50 μm, respectively. A-type particles account for up to ~70% of the iron oxide particles in FS and gradually decrease in abundance in downstream fly ashes, with only a trace amount in WA. B-type particles also show a similar decreasing pattern of from ~50% in BA to ~0% in WA. In contrast, C-type particles gradually increase in abundance from ~10% in BA to ~100% in WA. FS only contains low amounts of B- and C- types of iron oxide particles. Therefore, the distribution of the three types of iron oxide particles in the roasting wastes is consistent with the hypothesis that fine iron oxide particles migrated with the flue gas. Quantitative analyses of major elements indicated that, although the highest concentration of Fe was found in BA due to the preferential subsidence of heavy minerals in the boiler, substantial concentrations of Fe were also observed in the CA and WA, indicating that the signifi-

Table 3
Abundances of major elements in wall rocks, pyrite ores, and roasting wastes (mg/g).

Element	Wall rocks[a]				Pyrite ores[a]				FS	BA	CA	WA
	n[b]	Range	Median	Mean	n	Range	Median	Mean				
Al	11	1.27–75.2	54.5	45.3	5	0.05–22.1	22.1	13.4	35.2	24.9	34.6	30.2
Ca	11	0.71–10.0	1.07	3.9	5	1.29–10.2	10.2	6.68	30.2	17.9	14.2	15.7
Fe	11	4.27–16.4	7.89	6.91	5	150–475	150	277	340	470	420	438
K	11	0.75–25.2	4.31	11.9	5	0–7.55	7.55	4.53	12.6	7.94	8.15	8.8
Mg	11	0.30–10.9	1.8	4.15	5	0.03–4.02	4.02	2.5	6.93	3.96	3.31	3.87
Na	11	0.37–8.98	0.45	3.69	5	0–0.59	0.59	0.36	0.61	0.61	n.d.[c]	n.d.
Si	11	330–432	391.9	379	5	0–161	161	96.7	175	116	113	83
S	11	0.2–6.5	0.2	2.45	5	236–508	236	336	16.2	9.5	10.9	15.8

[a] Summarized from the data of this study and references [31] and [32].
[b] Number of measured samples.
[c] Not detectable.

Table 4
Abundances of trace elements in wall rocks, pyrite ores, and roasting wastes (μg/g).

Element	Wall rocks and gangue minerals[a]				Pyrite ores[a]				Clarke value[b]	FS	BA	CA	WA
	n[c]	Range	Median	Mean	*n*	Range	Median	Mean					
Cd	n.a.[d]	n.a.	n.a.	n.a.	2	0.27–2.06	1.17	1.17	0.15	8.77	10	32.7	14.8
Co	12	0.07–18.4	4.74	7.65	22	1.39–61.9	25.5	20.6	30	4.67	8.63	7.41	8.1
Cr	12	1.42–105	20.02	44.6	8	34.2–235	34.2	72.9	140	38.3	35.5	33.9	23.4
Mn	12	77.5–1007	310	490	5	897–3021	3021	2174	1100	3931	2132	1692	2552
Ni	12	23.8–111	28.33	36.7	22	21.7–68.0	39.5	38.2	90	18.6	26.4	19.3	22.1
Pb	9	33.3–603	245	269	7	813–11377	3865	4030	10	931	1184	2018	1699
Tl	n.a.	n.a.	n.a.	n.a.	22	1.9–56.4	4.8	11.7	0.53	44.7	49.6	51.1	70
Zn	12	1.91–2557	107.8	935	13	17.4–977	33.4	135	79	3295	3847	3438	3761

[a] Summarized from this study and references [21,22,33].
[b] Abundance in Earth crust; cited from [34].
[c] Number of measured samples.
[d] Not available.

cant proportion of iron oxides that are retained in fine particles still could escape from boiler.

Based on the above discussion, the pyrite transformations during the roasting must have been accompanied by significant particle fragmentation, which produced the fine particles in the flue gas. This fragmentation is related to S-release during the roasting [2] because the sizes of iron oxide particles are substantially correlated with the extent of pyrite combustion (see above). The porous structures and massive fissures observed in the larger iron oxide particles also are consistent with S-release playing an important role in this fragmentation.

The disappearance of calcite and the occurrence of gypsum in the wastes indicate that calcite has decomposed into calcium oxide, which subsequently reacted with sulfur oxides to formed gypsum. Aluminosilicate minerals exhibited high thermal stability through the roasting process although aluminosilicate glasses were occasionally observed in the roasting wastes. Physical fragmentation was the primary degradation process observed for quartz and aluminosilicates in the wastes: FS contains a significant amount of large-sized quartz and clay mineral particles, while mainly small, angular fragments of quartz and clay minerals were found in the three fly ashes. Si and Al having higher concentrations in FS than in fly ashes is consistent with that coarse particles of quartz and silicates being mainly retained in FS and only minor fine particles being emitted into flue gas. Amorphous limonite was mainly associated with gangue minerals, particularly clays, in the raw materials; a similar distribution was also observed in the roasting wastes, suggesting that limonite might have survived the roasting process.

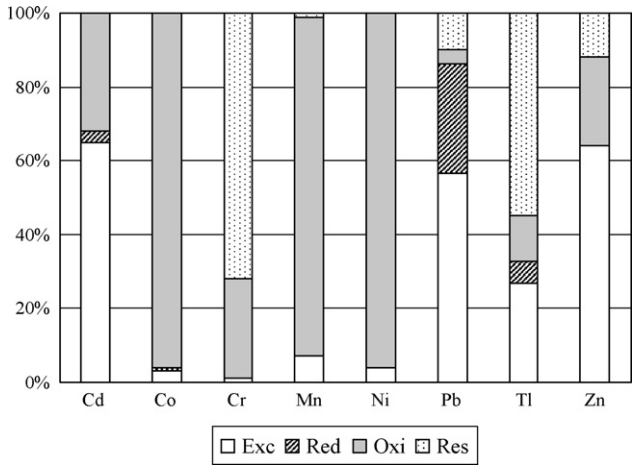

Fig. 2. Trace element partitioning in raw pyrite ores. Exc: acid exchangeable fraction; Red: easily reducible fraction; Oxi: oxidisable fraction; Res: residual fraction.

3.2. Transformations and partitioning of trace elements during the roasting of pyrite ores

The total concentrations of trace elements in raw pyrite ores, wall rocks and roasting wastes are summarized in Table 4. The results of the sequential extraction of the trace elements in raw pyrite ore are shown in Fig. 2 and expressed as percentages calculated as the proportion of one fraction concentration over the sum of all four fraction concentrations. This expression enables comparison among trace elements that are very different in concentration. The results of the sequential extraction of the trace elements in roasting wastes are shown in Fig. 3 and expressed as absolute concentrations in order to demonstrate the changes in element concentrations within each fraction between different roasting wastes. It should be noted that the rapid decrease of most of the studied elements in the first three fractions (i.e., Exc, Red, and Oxi) of WA may only signify that these fractions have been dissolved in and removed by the acidic washing water. On the other hand, the Res fraction in WA is comparable to Res fractions in other roasting wastes due to the high chemical stability of Res minerals in the acidic washing water.

3.2.1. Cadmium

Cadmium is enriched in pyrite ore (0.27–2.06 μg/g) compared with its Clarke value (0.15 μg/g). According to sequential extraction, Cd primarily occurred as Exc- and Oxi-Cd in pyrite ore, indicating that acid-exchangeable species and sulfides bound species are the main forms of Cd.

Cadmium showed an increasing trend from FS to CA and was significantly enriched in CA (32.7 μg/g), indicating that Exc- and Oxi-Cd in raw ores was partially liberated as vapor during the roasting. This is consistent with the thermodynamic prediction that Cd tends to vaporize as $Cd^0(g)$ and CdO(g) at the furnace temperature [35]. Significant enrichment of Cd in fly ashes was also observed in fuel and coal combustion studies [11,15,36,37]. Elements partially or fully vaporized during roasting usually undergo further transformations and partitioning downstream as the flue gas cools, including condensation, physical adsorption, chemisorptions or chemical reactions [38,39]. Sequential extraction results show that Cd mainly occurred as Res-Cd (>89%) in roasting wastes with only a minor amount associated with other fractions. In addition, Res-Cd showed lower concentration in FS and BA, but occurred at the highest level in CA (Fig. 3), in which relatively high Al was observed (Table 3). These observations indicated that gaseous Cd that has entered the downstream cleaning system primarily undergoes chemical reactions with aluminosilicates in the flue gas. Thermodynamic calculations predict that thermally stable compounds such as $CdO(SiO_2)$ and $CdO(Al_2O_3)$ may be formed from Cd-aluminosilicate interactions at temperatures of 600–1100 °C

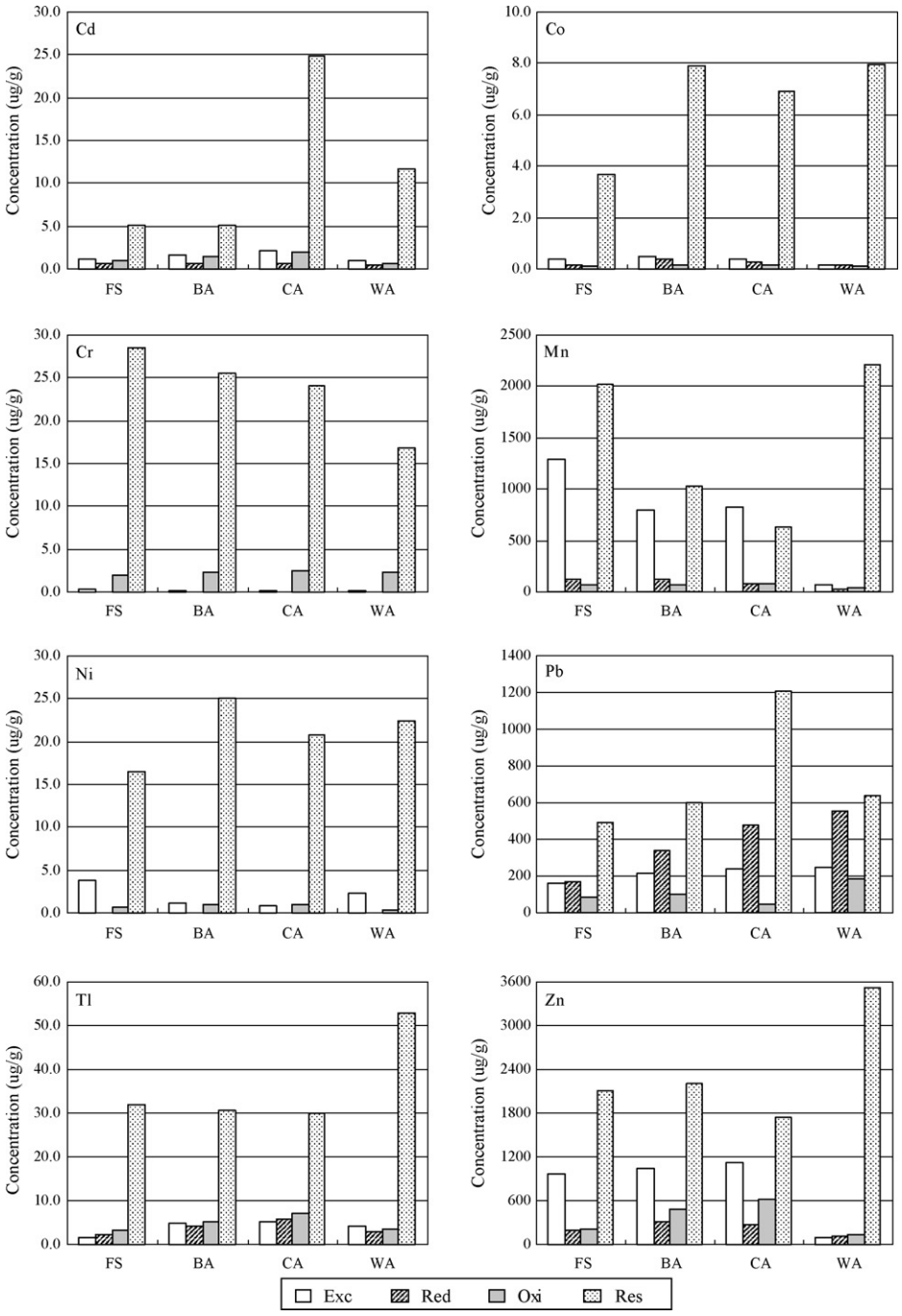

Fig. 3. Trace element partitioning in roasting wastes. Exc: acid exchangeable fraction; Red: easily reducible fraction; Oxi: oxidisable fraction; Res: residual fraction.

[40]. According to this prediction, the reactions between gaseous Cd and aluminosilicates in the flue gas accompanied volatilization of Cd during the roasting of pyrite ores in the fluidized bed furnace and resulted in the formation of fine Cd-aluminosilicate particles (i.e., Res-Cd). The large amount of aluminosilicate compounds present in the flue gas may have promoted the reactions between gaseous Cd and aluminosilicates. These Cd-containing particles subsequently migrated to, and mainly settled within, the cyclone scrubber. Previous studies have also observed the retention of Cd in fly ashes through chemical reactions between gaseous Cd and aluminosilicates [11,37].

Physical adsorption/condensation of gaseous species of trace elements on fly ash particles may result in an increasing trend in Exc fraction concentration with decreasing particle size because of preferential deposition on the fine particles [15]. Exc-Cd shows a slight increasing trend from FS to CA but only accounts for small amount of Cd in all roasting wastes, suggesting that simple physical adsorption/condensation on fine particles only have a minor effect on the deposition of gaseous Cd.

3.2.2. Cobalt and nickel

Cobalt and nickel have concentrations of <68 μg/g in pyrite ores and are mainly associated with sulfides (both at 96% in the Oxi fraction). Both Co and Ni do not show an increasing concentration downstream in the roasting wastes, reflecting their weak volatilities during the oxidation of Co- and Ni-bearing sulfides. This observation is consistent with the thermodynamic modeling result that Co and Ni would not vaporize from raw materials at 850 °C [35].

Weak volatilities of originally pyrite-associated Co and Ni were also observed during coal combustions [15,37]. In roasting wastes, Co and Ni are mainly present in the Res fraction (>79%), suggesting that most of sulfide-associated Co and Ni were incorporated into silicates or crystalline Fe-oxides during the roasting. Previous studies also suggested that Co and Ni could be easily incorporated into iron oxides via the formation of strong bonds during thermal treatments [15,42,43]. Moreover, thermodynamic analyses predict that $CoFe_2O_4$, $NiO{\cdot}Fe_2O_3$, and Fe_2NiO_4 will be major products of the reactions of Co or Ni with iron oxides [35,40]. In our study, the concentrations of Res-Co and Res-Ni are positively correlated with total Fe, but do not show any correlations with Si or Al, supporting the hypothesis that sulfides-associated Co and Ni in the pyrite ores were incorporated into iron oxides rather than silicates during the roasting. These Co- and Ni-bearing iron oxides would readily appear in fine particles, which dispersed into the flue gas and settled in the downstream zone as residual fraction.

3.2.3. Chromium

Chromium ranges from 34.2 to 235 μg/g with an average of 72.9 μg/g in the pyrite ores. Sequential extraction shows that Cr mainly occurred as Res-Cr (72%) in the pyrite ore, suggesting that silicates/crystalline minerals were the main hosts for Cr. In addition, 27% of Oxi-Cr was also detected in pyrite ore, showing that a significant amount of Cr is retained in sulfides as well.

Cr is enriched in FS and shows a decreasing concentration trend with decreasing particle size in roasting wastes (Table 4), indicating that Cr did not vaporize during the roasting. The non-volatility of Cr during the roasting of pyrite ores is consistent with predictions from the thermodynamic model [40]. However, high volatility of Cr was reported previously for coal/fuel combustions [10,36]. The discrepancy observed here between the combustions of pyrite ore and the coal/fuel may have been caused by the different forms of Cr in the raw materials. Previous studies indicated that ion-exchangeable or organic-associated Cr in coal or other fuels tends to be librated as gaseous species upon combustion, whereas Cr contained in silicates, non-soluble oxides and other minerals does not vaporize even at temperature >1000 °C [15,17]. As mentioned above, Cr is mainly retained in the silicates/crystalline minerals and sulfides of the pyrite ores and accordingly should not vaporize during roasting. In the roasting wastes, Cr is dominantly associated with silicates/crystalline minerals (>87% in Res; Fig. 3). Obviously, the Res-Cr was mainly derived from the large proportion of Cr retained in the initial silicates/crystalline minerals of the pyrite ores. In addition, Cr-bearing sulfides in the pyrite ores may have been significantly transformed into Cr-Fe-oxides (i.e., Res-Cr) along with sulfide oxidation [44]. Accordingly, the partitioning of Cr in the roasting wastes also supports the view that Res- and Oxi-Cr in the pyrite ores did not vaporize during the roasting process.

Since Cr mainly occurs with silicates/crystalline minerals in the pyrite ores, the fine particles of silicate/crystalline minerals from physical fragmentation during roasting would be the main form for Cr to be transported into the flue gas and the downstream cleaning system. The fine Cr-bearing Fe oxide particles generated from the sulfide oxidation should be important Cr-transportation vectors as well. Both of these two types of fine particles contributed the high concentrations of Res-Cr in the downstream wastes.

3.2.4. Manganese

Manganese is abundant in the pyrite ores (ranging from 897 to 3021 μg/g with an average of 2174 μg/g) and primarily occurred as Oxi-Mn (92%) with a small amount as Exc-Mn (7%), indicating that sulfides are the main hosts for Mn in the pyrite ores. Mn is enriched in FS but relatively depleted in fly ashes (Table 4), suggesting that Mn did not vaporize during the roasting process. This inference is also consistent with thermodynamic modeling that shows that Mn is not volatile at 850 °C [40]. However, previous studies on coal combustions offered different observations—either non-volatility of Mn (e.g., [20]) or significant volatility of Mn (e.g., [10]) was observed. The enhanced volatility of Mn during some coal combustions was probably caused by modes of Mn occurrence (e.g., carbonates, organic-bound) from which Mn could be easily liberated and by the high concentration of Cl in the coal [45], which could have resulted in the presence of abundant HCl in the flue gas greatly favoring the formation of gaseous Mn chlorides [40]. In contrast, the presence of abundant SO_2 in flue gas during the roasting of pyrite ores may have favored the formation of nonvolatile Mn sulfates [40].

The sequential extraction results show that Mn was mainly present as Res- (58%) and Exc-Mn (37%) in FS and only trace amounts of Red- (3%) and Oxi-Mn (2%) were found. This indicates that sulfide-associated Mn in the pyrite ores has oxidized and subsequently interacted with other minerals in the fluidized-bed furnace. Thermodynamic prediction suggests that thermostable Mn oxide species will initially form with stoichiometries such as MnO, Mn_3O_4, Mn_2O_3 and MnO_2, then other thermostable compounds such as $MnO{\cdot}Fe_2O_3$, $MnSiO_3$ and $MnO{\cdot}Al_2O_3$ will form through reactions with Fe, Si, and Al compounds if they are present in the thermal treatment system [40,41]. Obviously, the high proportion of Res-Mn in FS resulted from the formation of these thermostable compounds due to the presence of abundant iron oxides from pyrite oxidation (see Section 3.1) and silicates. However, the significant amount of Exc-Mn species in FS should be derived from Mn sulfates (see above). Exc-Mn species could also have resulted from the production of acid-soluble Mn oxides by insufficient reactions with Fe, Si, and Al compounds during the roasting probably due to the super high concentrations of Mn in the pyrite ores, low temperatures in the furnace, short residence time and/or other possible factors.

Significant amounts of Exc- (797 and 828 μg/g in BA and CA, respectively) and Res-Mn (1029 and 628 μg/g in BA and CA, respectively) were also observed in BA and CA, indicating that the Mn-bearing thermostable compounds mentioned above entered the flue gas as fine particles and settled with these particles in the downstream zone. Higher concentration of Res-Mn in WA could indicate that a large quantity of Mn migrated into the cleaning system as fine Mn-bearing iron oxides particles.

3.2.5. Lead

Lead is highly enriched in pyrite ores (ranging from 813 to 11377 μg/g with an average of 4030 μg/g) compared to its abundance in Earth's crust (i.e., Clarke value) which is only 10 μg/g. Lead is present mainly as Exc- (57%) and Red-Pb (30%) with minor as Res- (10%) and Oxi-Pb (4%) in the pyrite ores, indicating that acid-exchangeable species and Fe (hydr)oxides-bound species were the main forms of Pb in the pyrite ores, although galena, a significant Pb host, has been reported in the pyrite ores before [31]. The low proportion of Oxi-Pb in the studied pyrite ores could simply be caused by heterogeneity in the raw pyrite ores. On the other hand, galena weathering could also result in the low proportion of Oxi-Pb (and correspondingly high concentrations of Exc- and Red-Pb) observed in the examined pyrite ore because galena is readily weathered relative to other coexisting sulfides [46].

Lead is relatively depleted in FS (931 μg/g) but rich in fly ashes (up to 2018 μg/g; see Table 4), indicating that Pb in pyrite ores was liberated into the flue gas during roasting. This is consistent with the thermodynamic prediction that Pb tends to vaporize as PbO(g) and Pb^0(g) at the furnace temperature [35]. However, the substantial amount of Pb in the FS indicates that at least part of the Pb in the pyrite ores still did not vaporize. The partial volatilization of Pb has been also observed during coal and other combustions [10,15,36]. The non-volatilization of part of the Pb could be caused

by the occurrence of sulfur compounds and silicates with which Pb reacted to form condensed $PbSO_4$ and $PbO{\cdot}SiO_2$ [11].

Res- and Red-Pb dramatically increased in concentration from FS to CA, while Exc-Pb only showed a slight increase (Fig. 3). (i) Similar to Cd, the increasing trend of Res-Pb in fly ash from FS to CA was probably related to the formation of thermostable compounds through chemical reactions between gaseous Pb species and aluminosilicates in the flue gas [20,40,47,48]. The highest concentration of Res-Pb was in CA, which is the main zone in the cleaning system for settling fine aluminosilicates out of the flue gas (see Table 3), providing supporting evidence for this view. (ii) The increasing trend of Red-Pb in fly ashes from FS to WA implies that the chemical adsorption to Fe (hydr)oxides could also play an role in the deposition of gaseous Pb. In addition, the proportions of Red-Pb in pyrite ores and in roasting wastes are the highest of the studied trace elements, suggesting that initial Red-Pb may be retained through the roasting process because of the high thermostability of amorphous iron (hydr)oxides (see Section 3.1). (iii) As discussed for Cd, the slight increase of Exc-Pb from FS to CA indicates that, although it is not the primary mechanism for Pb to sink out of the flue gas, simple physical adsorption/condensation on fine particles also occurs. The high concentrations of sulfur compounds in the flue gas may have significantly enhanced the physical adsorption of gaseous Pb as condensed sulfate on the surface of fly ashes [40].

3.2.6. Thallium

Thallium is enriched in pyrite ores (ranging between 1.9–56.4 with an average of 11.7 μg/g) compared to its abundance in Earth crust, which is only 0.53 μg/g (Table 4). Tl is primarily retained as Res-Tl (55%), with the remainder mainly as Exc- (27%) and Oxi-Tl (12%), indicating that Tl in the pyrite ores is largely associated with silicates/crystalline minerals although some occurs as acid-exchangeable species and sulfides. As a lithophile and chalcophile element, Tl is readily enriched in silicates (e.g., micas) and sulfides (e.g., pyrite) in rocks [49]. Similar to the formation of acid-exchangeable Pb species in pyrite ores (see Section 3.2.5), the Exc-Tl in the pyrite ores could have partially derived from Tl-sulfide weathering.

Tl is relatively enriched in roasting wastes and a slight increase in Tl concentration is observed from FS to CA (Table 4), suggesting that Tl vaporized during the roasting. Gaseous Tl may have been derived from the liberation of Exc- and Oxi-Tl from the pyrite ores during roasting since a significant percentage decrease relative to pyrite ores is observed for these two fractions in FS (4% and 8% for Exc- and Oxi-Tl, respectively). Exc- and Red-Tl gradually increase in concentration from FS to CA, whereas Res-Tl shows a slight decrease (Fig. 3), indicating that gaseous Tl was deposited with the fly ashes mainly through physical adsorption/condensation or chemical adsorption on amorphous Fe (hydr)oxides rather than through chemical reactions with silicates or crystalline Fe-oxides. This is consistent with the thermodynamic prediction that there are no chemical reactions between gaseous Tl and Fe, Si, Al compounds in the flue gas [41].

A significant amount of Oxi-Tl is observed in the roasting wastes. The Oxi-Tl concentration increases from FS to CA, supporting the hypothesis that a significant amount of the Tl sulfides initially in the pyrite ores vaporized into the flue gas prior to oxidation. The high concentration of SO_2 in the roasting system may have facilitated the volatilization of Tl sulfides, as was observed for Zn by Frandsen et al. [35]. Rapid vaporization of trace element sulfides before or during the first combustion period has been reported in a previous study [16]. The relatively high volatility of Tl sulfides, as observed in this study, is probably related to its high sulfur affinity (where sulfur affinity is as follows: $Cr^{3+} < Mn^{2+} < Co^{2+} < Ni^{2+} < Zn^{2+} < Cd^{2+} < Tl^{+} < Pb^{2+}$). The higher the sulfur affinity of an element, the more stable its sulfides will be, and therefore the element is more likely to vaporize as a sulfide species.

On the other hand, a substantial concentration of Tl is also observed in the FS (44.7 μg/g), suggesting that much of the Tl did not vaporize during the roasting. Based on thermodynamic predictions, Tl should completely vaporize under oxidizing conditions at temperatures higher than 227 °C [41]. Strong volatilities of Tl in coal and biomass combustions have been observed [10,36,50]. The partial non-valorization of Tl observed here may be related to its modes of occurrence in the pyrite ores. Sequential extraction data indicate that Tl is primarily present as Res-Tl in the roasting wastes with only a small amount associated with other fractions. Res-Tl concentration is positively correlated with Si from FS to CA, indicating that silicate-associated species were the main forms of Res-Tl. Therefore, the initial silicate-Tl, the primary form of Tl in raw pyrite ores, could have been remained associated with silicates throughout roasting due to the high thermostability of the silicates and subsequently migrated as fine silicate particles (see discussion in Section 3.1). However, the highest concentration of Res-Tl is observed in WA, implying that part of the Tl (particularly sulfide-Tl) could have been incorporated into crystalline iron oxides during roasting and subsequently migrated downstream with the fine Fe oxide particles. Taken together, although Tl is a highly volatile element, the relatively high proportion of silicate-Tl in the pyrite ores and/or chemical reactions with Fe oxides may have limited Tl volatilization during roasting.

3.2.7. Zinc

Zinc occurs in the pyrite ores in concentration of 17.4–977 μg/g with an average of 135 μg/g and is primarily present as Exc- (64%) and Oxi-Zn (24%) with only minor amounts as Res-Zn (12%). The distribution of Zn indicates that acid exchangeable species and sulfides (e.g., sphalerite, pyrite) are the main forms of Zn in pyrite ores. Zn sulfides can be readily weathered to form hydrated Zn sulfates, carbonates or other acid-exchangeable species [46], which may have contributed to the Exc-Zn in the pyrite ores. The inferred modes of occurrence of Zn in the raw pyrite ores, based on the data from this study, may not exactly represent Zn occurrence in the roasted materials because the low concentration of Zn in the studied pyrite ores is not consistent with the enrichment of Zn observed in the roasting wastes (Table 4). However, Zn, primarily as sphalerite [31], is present in high concentrations (ranging from 1.91 to 2557 μg/g with an average of 935 μg/g) in the wall rocks and gangues, implying that lean ores incorporated into the roasted materials could be responsible for the discrepancy in Zn concentration between the raw pyrite ores and roasted wastes.

Zn is slightly enriched in fly ashes relative to FS (Table 4), indicating that Zn has weak volatility during roasting. Differing volatilities of Zn have been reported for coal or other combustions [10,15,17,36]. Bool and Helble [17] found that acid exchangeable Zn species in coals tend to volatilize, while sulfide-associated Zn species tend to oxidize with limited vaporization, and subsequently interact with other ash species during combustion at 1500 °C. In contrast, as suggested by the slight increase in Exc-Zn with decreasing particle size from FS to CA, only a small amount of Exc-Zn in the raw materials vaporized during roasting of the pyrite ores. One potential explanation for the difference in volatilities between this and other studies is that the weak volatility of Exc-Zn in this study actually reflects the incorporation of wall rocks and gangue minerals. Thus, the 64% Exc-Zn measured in the pyrite ore is not identical to the roasted materials because the proportion of sulfide-Zn (i.e., Oxi-Zn) in the roasted materials could have been greatly elevated by the addition of Zn sulfide-bearing wall rocks and gangue minerals. Another possibility, as supported by the high concentration of Exc-Zn in FS (976 μg/g), is that the weak volatility of Exc-Zn is simply caused by the lower roasting tem-

Table 5
Summary of trace element behaviors during roasting of pyrite ores in the sulfuric acid industry as inferred from this study, comparisons with thermodynamic predictions, and coal or other combustions in literature.

	Pyrite ore roasting in this study			Thermodynamic predication (850 °C) in literature: main transformation	Coal or other combustions in literature: main transformation
	Main partitioning in pyrite ores	Main transformation and emission in fluidized bed furnace (850 °C)	Migration and deposition in cleaning system		
Cd	Acid-exchangeable; Sulfide-bound	Vaporizes and mainly reacts with aluminosilicates in flue gas; mainly migrates as aluminosilicate-bound species and minor as gaseous species	Migrates by binding on aluminosilicates and settles in cyclone scrubber; gaseous species physically adsorb or condense on the surface of fine particles and gradually deposit	Vaporizes as $Cd^0(g)$ and CdO(g) [35,40]	Vaporizes at >1000 °C [15,37]; reacts with aluminosilicates in flue gas [11,48]
Co Ni	Sulfide-bound	Reacts with iron oxides during sulfide oxidation; mainly emit into flue gas with fine iron oxide particles	Migrates as iron oxide bound particles which mainly deposits in boiler and tower washer	Non-vaporize; reacts with iron oxides [35,40]	Pyrite-bound Co or Ni non-vaporizes at ~1000 °C [15,37]
Cr	Silicate-bound; Sulfide-bound	Detains in silicates for silicate-bound, or reacts with iron oxides for sulfide-bound during sulfide oxidation; mainly emits into flue gas with fine particles of silicates or iron oxides	Migrates as fine particles of silicates or iron oxides and gradually deposits	Non-vaporize [40]	Ion-exchangeable or organic-associated Cr vaporizes, but silicates- or non-soluble oxides-associated Cr not at ~1000 °C [15,17]
Mn	Sulfide-bound	Be oxidized into Mn oxides or further react with silicates and iron oxides or SO_2; emits into flue gas as fine particles	Migrates as fine particles of iron oxides, silicates, sulfate or Mn oxides and gradually deposits	Non-vaporize; Mn oxides or further reacts with silicates and iron oxides [40,41]	Have differing volatilities [10,20]
Pb	Acid-exchangeable; Fe-(hydr)oxide-bound	Vaporizes and mainly reacts with aluminosilicates in flue gas for acid-exchangeable Pb; detains in initial Fe (hydr)oxides for Fe (hydr)oxides-bound Pb; mainly migrates as aluminosilicates- and Fe (hydr)oxides-bound species with minor as gaseous species	Migrates by binding on aluminosilicates (deposits mainly in cyclone scrubber) and Fe (hydr)oxides (gradually deposits); gaseous species physically/chemically adsorb or condense on fine particles and gradually deposit	Vaporizes as PbO(g) and $Pb^0(g)$ [35,40]	Partially volatilizes [10,15,36]; reacts with aluminosilicates in flue gas [20,47,48]
Tl	Silicate-bound Acid-exchangeable Sulfide-bound	Vaporizes for acid-exchangeable and sulfide-bound Tl and emits as gaseous Tl species; reacts with iron oxides, then emitted into flue gas as fine iron oxides particles for sulfide-bound Tl; detain in silicates and emits as fine particles for silicates-bound Tl	Migrates as fine particles of iron oxides, silicates, and gradually deposits; gaseous species physically/chemically adsorb or condense on the surface of fine particles and gradually deposit;	Completely vaporizes [41]	Has high volatility [10,36,50]
Zn	Acid-exchangeable; Sulfide-bound	Vaporizes and emits into flue gas as gaseous Zn species; oxidized into oxides or further mainly reacts with iron oxides and emits into flue gas with fine iron oxide particles	Gaseous species physically adsorb or condense on the surface of fine particles and gradually deposit; same behavior as Mn for iron oxides-bound	Non-vaporizes; reacts with silicates [35,41]	Ion-exchanged Zn volatilizes; sulfide-bound species non-volatilizes [17]

perature of 850 °C which, in the presence of high concentrations of SO_2 [35], may have facilitated the formation of non-volatile $ZnSO_4$.

Res-Zn is the most abundant fraction in roasting wastes, which is not compatible with the low Res-Zn in the pyrite ores. The elevation of Res-Zn in the roasting wastes was probably caused by the reactions between Zn (in particular, sulfide-Zn) and iron oxides and/or silicates during roasting. The concentration of Res-Zn in the roasting wastes is positively correlated with the total iron (Table 3), suggesting that Zn in the roasted materials reacted with iron oxides during roasting and migrated into the flue gas as fine Zn-bearing iron oxide particles. Previous studies have reported the formation of stable $ZnO{\cdot}Fe_2O_3(s)$ through interactions between Zn and iron oxides [50]. The high concentration of iron oxides in the combustion system (Section 3.1) could have facilitated Zn and iron oxide interactions. In addition, thermodynamic models suggest that Zn could be retained in solid residues as thermostable ZnO (cr) or $ZnO{\cdot}Al_2O_3$ and $2ZnO{\cdot}SiO_2$ as a result of Zn-silicate interactions at 850 °C [19,35,41]. Therefore, the reactions between Zn and silicates cannot be excluded from this study, given the high concentration of silicates present during roasting.

Similar to Tl, Oxi-Zn is present in roasting wastes at a relatively high concentration which increased from FS to CA, suggesting that a significant amount of Zn sulfides vaporized prior to oxidation and subsequently migrated into the flue gas. The discussion in Section 3.2.6 for Oxi-Tl is applicable to Oxi-Zn as well.

Studies of thermal treatments suggest that the total concentration of a semivolatile element should increase with decreasing waste particle size due to preferential adsorption on the surface of fine particles [14–16]. In this study, the total concentration of Zn does not increase with decreasing waste particle size. However, the volatility of Zn still can be inferred from the concentrations of Exc-Zn and Oxi-Zn, which do increase with decreasing waste particle size. Accordingly, one should be cautious to address the

volatility of an element during a thermal treatment with only total concentration pattern in wastes.

4. Summary

In order to better constrain the potential environmental hazards posed by trace element by-products of the sulfuric acid industry, the transformations and partitioning of Cd, Co, Cr, Mn, Ni, Pb, Tl, and Zn during the roasting of pyrite ores in a functioning sulfuric acid plant were investigated, primarily through analyses of trace element concentrations and chemical partitioning in both pyrite ores and corresponding roasting wastes. The raw materials used for sulfuric acid production at the studied plant were mainly composed of pyrite with minor amounts of quartz, clays, carbonates and limonite. During roasting, pyrite was oxidized to hematite and magnetite, the fine fragments of which readily migrated into the fly ashes. Refractory minerals, such as quartz and clays, underwent physical fragmentation during roasting, and were mainly retained in bottom slag. Carbonates decomposed into oxides and were retained with silicates in the bottom slag. Limonite was also stable through roasting and was mainly retained in the bottom slag. Accompanying these mineral transformations, the eight studied trace elements demonstrated very different transformations and partitioning behaviors, as summarized in Table 5. For comparison, a literature review of the thermodynamic predictions and behaviors during coal combustion of each trace element are also given in Table 5.

The conclusions that can be drawn from this research are:

(i) The mode of occurrence of trace elements in pyrite ores and the thermostability of subsequently formed trace element-bearing species played major roles in the transformations of the selected trace elements during roasting. Those elements associated with amorphous iron (hydr)oxides (e.g., Pb) and silicates/crystalline minerals (e.g., Cr) were nonvolatile and mainly retained in the initial solid phases. Those elements that were present in acid-exchangeable species (Cd, Pb, Tl and Zn) or associated with sulfides (Co, Mn, and Ni) in pyrite ores were readily liberated during the roasting. Elements that tend to form species with low thermostabilities (Cd, Pb, and Tl) were primarily vaporized, while elements that tend to form species with high thermostabilities (Co, Mn, and Ni) mainly reacted with other minerals which then remained in the solid residues. Due to the high concentrations of sulfur compounds (mainly as SO_2) in the roasting system, some of the semivolatile trace element (e.g., Tl and Zn) sulfides were able to directly vaporize and then condensed on the fly ash particles during cooling of the flue gas.

(ii) The volatility of trace elements had a significant effect on their partitioning in the roasting wastes. Nonvolatile elements (Co, Cr, Mn, and Ni) were mainly retained in the bottom slag and could migrate into the flue gas only *via* fine, trace element-bearing particles. The partitioning of these particle-bound elements in the roasting wastes was determined by settling of the particles during cooling of the flue gas; distribution of the trace element fractions was not correlated with the particle size distribution of the roasting wastes. Semivolatile elements (Cd, Pb, Tl and Zn) were primarily vaporized and emitted into the flue gas as gaseous species. Once in the vapor phase, these gaseous species physically adsorbed or condensed onto particle surfaces (Cd, Zn, Pb, and Tl), chemically adsorbed onto amorphous iron (hydr)oxides (Pb and Tl), or reacted with Fe, Si, and Al compounds (Pb and Cd). The partitioning of these semivolatile elements was determined by the adsorption behavior of their gaseous species.

(iii) The volatilities of Cd and Pb are similar to those observed in coal combustions but lower than those predicted by thermodynamic calculations. The reactions of their gaseous species with silicates in the roasting system are responsible for their reduced volatilities. The volatilities of Tl and Cr are lower than those in coal and other types of combustions as well as in thermodynamic predictions, probably due to their significant association with the silicates/crystalline minerals of the pyrite ores. The volatility of Mn is similar to that predicted by thermodynamic calculations, but lower than the volatility observed in coal and other types of combustions, probably because of its major association with sulfides in the raw ores and its reactions with iron oxides and silicates during roasting. The observed volatility of Zn is higher than in thermodynamic predictions, but lower than those of the coal and other types of combustions, probably due to its predominant association with sulfides and acid-exchangeable factions, and its reactions with iron oxides and silicates during roasting. The behaviors of Co and Ni during roasting are consistent with other studies.

Since the analyses were conducted on samples from a real pyrite roasting plant, it is difficult to completely exclude the possibility of unknown variables from the industrial process itself affecting the transformations and partitioning behaviors of the trace elements observed in this study. Thus, one should be aware that the inferences drawn from the observations of this study cannot simply equate to those drawn from research into the fundamental science of trace element transformations and partitioning during the pyrite roasting process.

Acknowledgements

The authors wish to thank C. Xie, X. Tu, H. Zhang and C. Yu for technical assistance, and W. Xie of Guangzhou University for their constructive comments and suggestions. This project was supported by The United Foundation of National Nature Science Foundation Committee of P.R. China and Guangdong Provincial Government (no. U0633001).

References

[1] D.A. Spears, M.R. Martinez Tarazona, S. Lee, Pyrite in UK coals: its environmental significance, Fuel 73 (1994) 1051–1055.
[2] S. Srinivasachar, J.J. Helble, A.A. Bonim, Mineral behavior during coal combustion 1. pyrite transformations, Prog. Energy Combust. Sci. 16 (1990) 281–292.
[3] G. Hu, K. Dam Johansen, S. Wedel, J.P. Hansen, Decomposition and oxidation of pyrite, Prog. Energy Combust. Sci. 32 (2006) 295–314.
[4] Z. Lin, U. Qvarfort, Predicting the mobility of Zn, Fe, Cu, Pb, Cd from roasted sulfide (pyrite) residues—a case study of wastes from the sulfuric acid industry in Sweden, Waste Manage. 16 (1996) 671–681.
[5] M. Benvenuti, I. Mascaro, F. Corsini, P. Lattanzi, P. Parrini, G. Tanelli, Mine waste dumps and heavy metal pollution in abandoned mining district of Boccheggiano (Southern Tuscany, Italy), Environ. Geo. 30 (1997) 238–243.
[6] M. Thiry, S. Huet Taillanter, J.M. Schmitt, The industrial waste land of Mortagne-du-Nord (59)-I-Assessment, composition of the slags, hydrochemistry, hydrology and estimate of the outfluxes, Bulletin De La Societe Geologique De France 173 (2002) 369–381.
[7] M.A. García, J.M. Chimenos, A.I. Fernández, L. Miralles, M. Segarra, F. Espiell, Low-grade MgO used to stabilize heavy metals in highly contaminated soils, Chemosphere 56 (2004) 481–491.
[8] C. Yang, Y. Chen, P. Peng, C. Li, X. Chang, C. Xie, Distribution of natural and anthropogenic thallium in the soils in an industrial pyrite slag disposing area, Sci. Total Environ. 341 (2005) 159–172.
[9] E.I.B. Chopin, B.J. Alloway, Trace element partitioning and soil particle characterization around mining and smelting areas at Tharsis, Riotinto and Huelva, SW Spain, Sci. Total Environ. 373 (2007) 488–500.
[10] B. Miller, D.R. Dugwell, R. Kandiyoti, Partitioning of trace elements during the combustion of coal and biomass in a suspension-firing reactor, Fuel 81 (2002) 159–407.
[11] M. Belén Folgueras, R.M. Diaz, J. Xiberta, I. Prieto, Volatilisation of trace elements for coal-sewage sludge blends during their combustion, Fuel 82 (2003) 1939–1948.

[12] B. Miller, D.R. Dugwell, R. Kandiyoti, The fate of trace elements during the Co-combustion of wood-bark with waste, Energy Fuels 20 (2006) 520–531.
[13] A.L. Elled, L.E. Amand, B. Leckner, B.A. Andersson, The fate of trace elements in fluidized bed combustion of sewage sludge and wood, Fuel 86 (2007) 843–852.
[14] L.B. Clarke, The fate of trace elements during coal combustion and gasification: an overview, Fuel 72 (1993) 731–736.
[15] K.C. Galbreath, D.L. Toman, C.J. Zygarlicke, J.H. Pavlish, Trace element partitioning and transformations during combustion of bituminous and subbituminous U.S. coals in a 7-kW combustion system, Energy Fuels 14 (2000) 1265–1279.
[16] M. Xu, R. Yan, C. Zheng, Y. Qiao, J. Han, C. Sheng, Status of trace element emission in a coal combustion process: a review, Fuel Process. Technol. 85 (2003) 215–237.
[17] L.E. Bool III, J.J. Helble, A laboratory study of the partitioning of trace elements during pulverized coal combustion, Energy Fuels 9 (1995) 880–887.
[18] X. Querol, R. Juan, A. Lopez Soler, J.L. Fernandez Turiel, C.R. Ruiz, Mobility of trace elements from coal and combustion wastes, Fuel 75 (1996) 821–838.
[19] B. Miller, D.R. Dugwell, R. Kandiyoti, The Influence of injected HCl and SO_2 on the behavior of trace elements during wood-bark combustion, Energy Fuels 17 (2003) 1382–1391.
[20] Y. Huang, B. Jin, Z. Zhong, R. Xiao, Z. Tang, H. Ren, Trace elements (Mn, Cr, Pb, Se, Zn, Cd and Hg) in emissions from a pulverized coal boiler, Fuel Process. Technol. 86 (2004) 23–32.
[21] B. Marin, M. Valladon, M. Polve, A. Monaco, Reproducibility testing of a sequential extraction scheme for the determination of trace metal speciation in a marine reference sediment by inductively coupled plasma-mass spectrometry, Anal. Chim. Acta 342 (1997) 91–112.
[22] V. Balaram, Assessment of the ICP-MS method using the interlaboratory QA study of two Polish soil RMs, Accred. Qual. Assur. 5 (2000) 325–330.
[23] A.M. Ure, Ph. Quevauviller, H. Muntau, B. Griepink, Speciation of heavy metals in solids and harmonization of extraction techniques undertaken under the auspices of the BCR of the Commission of the European Communities, Int. J. Environ. Anal. Chem. 51 (1993) 135–142.
[24] C. Yang, Y. Chen, P. Peng, C. Li, X. Chang, C. Xie, The study of the sequential extraction procedure for thallium in soils, J. Instrum. Anal. (China) 24 (2005) 1–6.
[25] C.M. Davidson, P.C.S. Ferreira, A.M. Ure, Some sources of variability in application of the three-stage sequential extraction procedure recommended by BCR to industrially-contaminated soil, Fresenius J. Anal. Chem. 363 (1999) 446–451.
[26] K.F. Mossop, C.M. Davidson, Comparison of original and modified BCR sequential extraction procedures for the fractionation of copper, iron, lead, manganese and zinc in soils and sediments, Anal. Chim. Acta 478 (2003) 111–118.
[27] R.A. Sutherland, F.M.G. Tack, Determination of Al, Cu, Fe, Mn, Pb and Zn in certified reference materials using the optimized BCR sequential extraction procedure, Anal. Chim. Acta 454 (2002) 249–257.
[28] C.M. Davidson, A.S. Hursthouse, D.M. Tognarelli, A.M. Ure, G.J. Urquhart, Should acid ammonium oxalate replace hydroxylammonium chloride in step 2 of the revised BCR sequential extraction protocol for soil and sediment? Anal. Chim. Acta 508 (2004) 193–199.
[29] C. Yuan, J. Shi, H. Bin, J. Liu, L. Liang, G. Jiang, Speciation of heavy metals in marine sediments from the East China Sea by ICP-MS with sequential extraction, Environ. Int. 30 (2004) 769–783.
[30] O. Mestek, R. Koplík, H. Fingerová, M. Suchánek, Determination of thallium in environmental samples by inductively coupled plasma mass spectrometry: comparison and validation of isotope dilution and external calibration methods, J. Anal. Spectrom. 15 (2000) 403–407.
[31] J. Pan, Q. Zhang, B. Zhang, A preliminary discussion on geochemical characteristics and genesis of the Dajiangping Pyrite Deposit, Western Guangdong, Miner. Dep. (China) 13 (1994) 231–241.
[32] D. Chen, G. Chen, J. Pan, S. Ma, W. Dong, J. Gao, X. Chen, Characteristics of the hydrothermal sedimentation of the Dajiangping Superlarge Pyrite Deposit, in Yunfu, Guangdong, Geochimica (China) 27 (1998) 12–19.
[33] W. Xie, Y. Chen, S. Chen, Distribution of thallium in pyrite ores and its cinders of Yunfu Pyrite Mine, Guangdong, Multipurpose Utilization Miner. Resourc. (China) (2) (2001) 23–25.
[34] "Abundance in Earth's Crust". <http://www.webelements.com/periodicity/abundance_crust/> (Accessed 2007).
[35] F. Frandsen, K. Dam Johansen, P. Rasmussen, Trace elements from combustion and gasification of coal-an equilibrium approach, Prog. Energy Combust. Sci. 20 (1994) 115–138.
[36] E. Häsänen, L. Aunela-Tapola, V. Kinnunen, K. Larjava, A. Mehtonen, T. Salmikangas, J. Leskelä, J. Loosaar, Emission factors and annual emissions of bulk and trace elements from oil shale fueled power plants, Sci. Total Environ. 198 (1997) 1–12.
[37] R. Yan, X. Lu, H. Zeng, Trace elements in Chinese coals and their partitioning during coal combustion, Combust. Sci. Technol. 145 (1999) 57–81.
[38] J.A. Ratafia-Brown, Overview of trace element partitioning in flames and furnaces of utility coal-fired boilers, Fuel Process. Technol. 39 (1994) 139–157.
[39] M. Xu, R. Yan, C. Zheng a, Y. Qiao, J. Han, C. Sheng, Status of trace element emission in a coal combustion process: a review, Fuel Process. Technol. 85 (2003) 215–237.
[40] M. Dı'az Somoano, S. Unterberger, K.R.G. Hein, Prediction of trace element volatility during co-combustion processes, Fuel 85 (2006) 1087–1093.
[41] R. Yan, D. Gauthier, G. Flamant, Partitioning of trace elements in the flue gas from coal combustion, Combust. Flame 125 (2001) 942–954.
[42] R.M. Cornell, R. Giovanoli, Effect of cobalt on the formation of crystalline iron-oxides from ferrihydrite in alkaline media, Clays Clay Miner. 37 (1989) 65–70.
[43] S. Music, S. Popovic, S. Dalipi, Formation of oxide phases in the system Fe_2O_3–NiO, J. Mater. Sci. 28 (1993) 1793–1798.
[44] S. Music, S. Popovic, M. Ristic, Chemical and structural-properties of the system Fe_2O_3–Cr_2O_3, J. Mater. Sci. 28 (1993) 632–638.
[45] S.V. Vassilev, C.G. Vassileva, Geochemistry of coals, coal ashes and combustion wastes from coal-fired power stations, Fuel Process. Technol. 51 (1997) 19–45.
[46] L. Cui, X. Chen, X. Xu, J. Feng, T. Chen, Simulation experiments on weathering and oxidation of sulfide minerals in mine tailings, Acta Petrologica et Mineralogica (China) 3 (2002) 298–302.
[47] M.V. Scotto, M. Uberoi, T.W. Peterson, F. Shadman, J.O.L. Wendt, Metal capture by sorbents in combustion processes, Fuel Process. Technol. 39 (1994) 357–372.
[48] W.P. Linak, K. Srivastava, J.O.L. Wendt, Sorbent capture of nickel, lead and cadmium in a laboratory swirl flame incinerator, Combust. Flame 100 (1995) 241–250.
[49] J.O. Nriagu, History, production, and uses of thallium, in: J.O. Nriagu (Ed.), Thallium in the Environment, Wiley-Interscience, New York, 1998, pp. 7–8.
[50] M.B. Folgueras, R.M. Dı'az, J. Xiberta, I. Prieto, Volatilisation of trace elements for coal–sewage sludge blends during their combustion, Fuel 82 (2003) 1939–1948.